

# Removal of Stratospheric O<sub>3</sub> by Radicals: In Situ Measurements of OH, HO<sub>2</sub>, NO, NO<sub>2</sub>, ClO, and BrO

P. O. Wennberg,\* R. C. Cohen, R. M. Stimpfle, J. P. Koplow, J. G. Anderson, R. J. Salawitch, D. W. Fahey, E. L. Woodbridge, E. R. Keim, R. S. Gao, C. R. Webster, R. D. May, D. W. Toohey, L. M. Avallone, M. H. Proffitt, M. Loewenstein, J. R. Podolske, K. R. Chan, S. C. Wofsy

Simultaneous in situ measurements of the concentrations of OH, HO<sub>2</sub>, ClO, BrO, NO, and NO<sub>2</sub> demonstrate the predominance of odd-hydrogen and halogen free-radical catalysis in determining the rate of removal of ozone in the lower stratosphere during May 1993. A single catalytic cycle, in which the rate-limiting step is the reaction of HO<sub>2</sub> with ozone, accounted for nearly one-half of the total O<sub>3</sub> removal in this region of the atmosphere. Halogen-radical chemistry was responsible for approximately one-third of the photochemical removal of O<sub>3</sub>; reactions involving BrO account for one-half of this loss. Catalytic destruction by NO<sub>2</sub>, which for two decades was considered to be the predominant loss process, accounted for less than 20 percent of the O<sub>3</sub> removal. The measurements demonstrate quantitatively the coupling that exists between the radical families. The concentrations of HO<sub>2</sub> and ClO are inversely correlated with those of NO and NO<sub>2</sub>. The direct determination of the relative importance of the catalytic loss processes, combined with a demonstration of the reactions linking the hydrogen, halogen, and nitrogen radical concentrations, shows that in the air sampled the rate of O<sub>3</sub> removal was inversely correlated with total NO<sub>x</sub> loading.

The response of stratospheric ozone to chemical, thermal, or radiative perturbations depends to first order on which catalytic cycles dominate the rate of O<sub>3</sub> destruction, which processes link the nitrogen, hydrogen, and halogen radical families, and how these changes affect stratospheric transport. For two decades, it was thought that nitrogen radicals [NO and NO<sub>2</sub> (NO<sub>x</sub>)] dominated the catalytic destruction of ozone in the middle and lower stratosphere with secondary contributions from the odd-hydrogen radicals [OH and HO<sub>2</sub> (HO<sub>x</sub>)] and minor contributions from chlorine and bromine radicals (ClO and BrO). The expected predominance of the nitrogen oxides directly influenced the scientific and political debates over the environmental impact

of chlorofluorocarbons and supersonic commercial aviation; nitrogen oxide effluent from supersonic transports (SSTs) was expected to lead to significant O<sub>3</sub> loss, whereas the influence of halogen chemistry was expected to be isolated to higher altitudes (30 to 50 km). Recent in situ observations (1) as well as modeling work (2) have shed considerable doubt on this model. In particular, these efforts have demonstrated the important role that heterogeneous chemistry plays in the removal of NO<sub>x</sub> in the lower stratosphere.

The Stratospheric Photochemistry, Aerosols and Dynamics Expedition (SPADE) aircraft measurement campaign was designed explicitly to investigate the photochemistry of the mid-latitude lower stratosphere. Nine flights originating from the National Aeronautics and Space Administration (NASA) Ames Research Center (37°N, 122°W) were made in late April and May 1993 to investigate the atmosphere up to 21 km between 15° and 60°N latitude. The NASA ER-2 payload was augmented from that flown in the Airborne Arctic Stratospheric Expedition II (AASE II) deployment (3) with instruments to measure the concentrations of OH, HO<sub>2</sub>, NO<sub>2</sub>, and CO<sub>2</sub>, as well as the ultraviolet (UV) and visible radiation field. The measurements were made during a time when record low values of global O<sub>3</sub> were ob-

served (4). The expedition was designed as part of a NASA program to assess the potential impact of commercial supersonic aircraft on stratospheric O<sub>3</sub> (5).

The SPADE measurements included characterization of the diurnal dependence of the free-radical concentrations as well as vertical concentration profiles from various latitudes. We used these measurements to calculate the diurnally averaged photochemical removal rate of O<sub>3</sub>. The data show that the hydrogen and halogen radicals dominated destruction of O<sub>3</sub> in the mid-latitude lower stratosphere in May 1993. The nitrogen radicals were found to contribute less than 20% to the total catalytic loss rate between 16 and 20 km.

The extensive data set, including measurements of the concentrations of long-lived species such as O<sub>3</sub>, H<sub>2</sub>O, N<sub>2</sub>O, and CO<sub>2</sub>, obtained during SPADE also allows a quantitative test of our understanding of the processes that couple the odd hydrogen and halogen radicals to the concentrations of NO<sub>x</sub>. In particular, we could examine the response of [HO<sub>2</sub>] and [ClO] with respect to variations in [NO] and [NO<sub>2</sub>] while accounting for changes in the chemical, dynamical, and meteorological properties of the sampled air. We show that the concentrations of HO<sub>2</sub> and ClO were inversely correlated with those of NO and NO<sub>2</sub>. As a direct consequence of this coupling and the relative importance of the various catalytic processes, the photochemical removal rate of O<sub>3</sub> in the air masses sampled during the SPADE campaign was inversely correlated with the concentration of NO<sub>x</sub>.

**New measurements of radicals: OH, HO<sub>2</sub>, and NO<sub>2</sub>.** The importance of hydrogen radicals to the chemical structure of the atmosphere was first considered by Bates and Nicolet (6). OH and HO<sub>2</sub> are present in the lower stratosphere at mixing ratios (7) in the part per trillion by volume range (pptv) [see, for example, Stimpfle *et al.* (8)]. Prior to the SPADE campaign, however, OH and HO<sub>2</sub> concentrations had not been measured simultaneously with those of NO<sub>x</sub> and ClO<sub>x</sub>—a requirement for constraining the relative importance of the catalytic cycles. Details of the new instrumentation for HO<sub>x</sub> are described elsewhere (9). Briefly, air is brought into the nose of the aircraft through a flow system designed to provide boundary-layer-free sampling. [OH] is measured by laser-induced fluorescence using the Q<sub>1</sub>(2) and Q<sub>21</sub>(2) rotational lines of the A<sup>2</sup>Σ<sup>+</sup> (v = 1) ← X<sup>2</sup>Π (v = 0) electronic transition near 282 nm. Collisions with air quench the vibration in the excited state and red-shifted fluorescence (309 nm) is observed. The laser light is produced by a dye laser with a high pulse-repetition rate powered by diode-laser pumped Nd<sup>3+</sup>:YLF lasers. Precise measurements are obtained

P. O. Wennberg, R. C. Cohen, R. M. Stimpfle, J. P. Koplow, and J. G. Anderson are with the Department of Chemistry, Harvard University, 12 Oxford Street, Cambridge, MA 02138, USA. R. J. Salawitch and S. C. Wofsy are with the Division of Applied Sciences and Department of Earth and Planetary Sciences, Harvard University, Cambridge, MA 02138, USA. D. W. Fahey, E. L. Woodbridge, E. R. Keim, R. S. Gao, and M. H. Proffitt are with the National Oceanic and Atmospheric Administration Aeronomy Laboratory, Boulder, CO 80303, USA. C. R. Webster and R. D. May are with the Jet Propulsion Laboratory, Pasadena, CA 91109, USA. D. W. Toohey and L. M. Avallone are with Earth System Science, University of California, Irvine, CA 92717, USA. M. Loewenstein, J. R. Podolske, and K. R. Chan are with the National Aeronautics and Space Administration Ames Research Center, Moffett Field, CA 94035, USA.

\*To whom correspondence should be addressed.

with this technique; OH mixing ratios as low as 0.1 pptv can be determined with a signal-to-noise ratio of greater than 5 in a few seconds of observation. The absolute experimental uncertainty is estimated to be  $\pm 20\%$  ( $1\sigma$  confidence intervals are used throughout this article). HO<sub>2</sub> is measured after chemical conversion to OH by the fast gas-phase reaction with NO. Absolute uncertainty in the HO<sub>2</sub> concentration, which includes the uncertainty in the calibration of the instrument for OH, is  $\sim 25\%$ .

The vertical profile of [OH] measured between 20° and 60°N latitude is shown in Fig. 1. To account for differences in solar illumination, the data are normalized to 30° solar zenith angle (SZA) with an empirical expression derived below. With the exception of its dependence on SZA and altitude, the OH concentration is remarkably invariant in the lower stratosphere. The trace gases that are thought to control the OH concentration [O<sub>3</sub> and the reactive odd nitrogen species (NO<sub>x</sub>) such as nitric acid] vary greatly over this latitude range. The lack of variance reflects the coincidental balancing of changes in the OH production and loss rates as a function of variations in the source gases and sinks (10).

Two different measurements of [NO<sub>2</sub>] were made during SPADE. The Jet Propulsion Laboratory (JPL) Aircraft Laser IR Absorption Spectrometer provided NO<sub>2</sub> data every 5 min for portions of some flights (11). A tunable diode laser is modulated over a few tenths of wave numbers near 1633 cm<sup>-1</sup> so that long-path absorption of two of the vibration-rotation transitions in the  $\nu_3$  band is observed in a multipass flow cell. Accuracy, which varies from flight to flight, is estimated to be 15% for concentrations of 400 pptv, decreasing to  $\pm 25\%$  for concentrations below 100 pptv.

[NO<sub>2</sub>] measurements were also obtained by the National Oceanic and Atmospheric Administration (NOAA) Reactive Nitrogen Instrument (12). A metal halogen-doped Hg lamp is used to dissociate  $\sim 65\%$  of the NO<sub>2</sub>. The NO fragment is then measured by chemiluminescence after reaction with O<sub>3</sub>. Accuracy is estimated to be  $\pm 30\%$  during daytime. During nighttime, the absence of ambient NO in the signal reduces the uncertainty to  $\pm 10\%$ .

**The diurnal behavior of free radicals.** The chemical removal of O<sub>3</sub> is slow in the lower stratosphere. In a given air parcel, changes in the mixing ratio of O<sub>3</sub> occur on time scales of months (except for regions over the Antarctic during late winter where chlorine and bromine radicals reduce the O<sub>3</sub> lifetime to a few weeks). In contrast, the chemistry of the free radicals is fast; variations in the concentrations of the radicals reflect primarily the changes in solar illumination. Although instantaneous O<sub>3</sub> removal

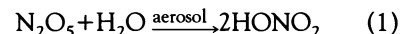
rates can be calculated directly from the radical measurements, determination of the diurnally averaged rates requires a characterization of their concentrations during a 24-hour period. Such a measurement is difficult to obtain from an aircraft because movement of air can result in variations in the chemical properties of the air masses sampled.

To have the best opportunity of sampling similar air masses during a 2-day period, flights were scheduled for May to coincide with the transition of the stratospheric circulation from predominantly westerlies to easterlies ("turn-around"). Forecasts of stratospheric winds were used to orient the level flight track perpendicular to the mean flow and to avoid thermal disturbances associated with mountain-forced gravity waves. This flight plan allowed investigation of the diurnal dependence of the free-radical concentrations.

The measured mixing ratios of NO<sub>2</sub>, NO, ClO, HO<sub>2</sub>, and OH during the flights of the morning of 11 May and afternoon of 12 May 1993 are shown in Fig. 2. In situ measurements of the tracers O<sub>3</sub>, CO<sub>2</sub>, H<sub>2</sub>O, and N<sub>2</sub>O confirm the dynamical and chemical similarity of the air sampled on these 2 days at an altitude of  $\sim 19$  km.

With the exception of NO<sub>2</sub>, all of the observed radicals are produced photolytically each day and their concentrations fall to zero during the night. The diurnal dependence of each radical species reflects the spectral properties of the source gases. NO is produced primarily from the photolysis of NO<sub>2</sub> at wavelengths longer than 320 nm. Because the atmosphere is nearly nonabsorptive at these wavelengths (O<sub>3</sub> does not attenuate this radiation) the photolysis rate

of NO<sub>2</sub> is nearly constant between sunrise and sunset. Thus, the diurnal shapes are either relatively flat-topped (NO) or -bottomed (NO<sub>2</sub>). The small enhancement in the concentration of NO<sub>x</sub> observed between sunrise and sunset is primarily a result of the photolysis of nitric acid (HONO<sub>2</sub>) and reaction of OH with HONO<sub>2</sub>. NO<sub>x</sub> is recycled to HONO<sub>2</sub> through the reaction of OH with NO<sub>2</sub> during the day and at night by the formation and subsequent hydrolysis of N<sub>2</sub>O<sub>5</sub> on sulfuric acid aerosols:



In the absence of aerosols, [N<sub>2</sub>O<sub>5</sub>] builds up over the night and is photolyzed back to NO<sub>x</sub> during the day (13).

The model of [NO] and [NO<sub>2</sub>] in Fig. 2 (shown as a solid line) is produced by setting the NO<sub>x</sub> concentration to 600 pptv at noon, based on the observations of [NO] and [NO<sub>2</sub>], and calculating the change in [NO<sub>x</sub>] by integrating the important production and loss processes (14). The partitioning between NO and NO<sub>2</sub> is then calculated by assuming they are in photochemical steady state (15):

$$\frac{[\text{NO}_2]}{[\text{NO}]} \text{ (steady state) } = 0.7 \times \frac{\{k_{\text{NO}+\text{O}_3}[\text{O}_3] + k_{\text{NO}+\text{ClO}}[\text{ClO}] + k_{\text{NO}+\text{HO}_2}[\text{HO}_2]\}}{J_{\text{NO}_2}} \quad (2)$$

where  $k_{\text{NO}+\text{O}_3}$ ,  $k_{\text{NO}+\text{ClO}}$ , and  $k_{\text{NO}+\text{HO}_2}$  are the bimolecular rate constants for the formation of NO<sub>2</sub> from the reactions of NO with O<sub>3</sub>, ClO, and HO<sub>2</sub>. The photolysis rate of NO<sub>2</sub>,  $J_{\text{NO}_2}$ , is calculated from a ra-

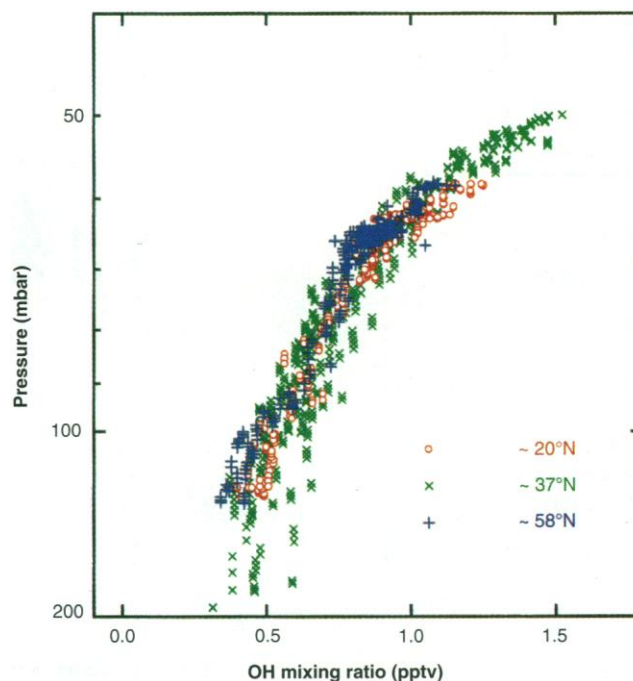


**Fig. 1.** Altitude profiles of [OH] measured during the SPADE campaign. The data have been normalized to 30° SZA by using the measured diurnal behavior. Despite the large increase in the concentrations of O<sub>3</sub> and NO<sub>x</sub> observed between 20° and 60°N latitude, little variation in [OH] is observed at a given altitude.

diation model that accounts for Rayleigh and aerosol scattering, which is constrained by the measurements of column  $O_3$  and albedo by the Total  $O_3$  Mapping Spectrometer (TOMS) (16).  $NO_2$  observations from the NOAA instrument are available only for the flight of 12 May (shown in Fig. 2) when measurements

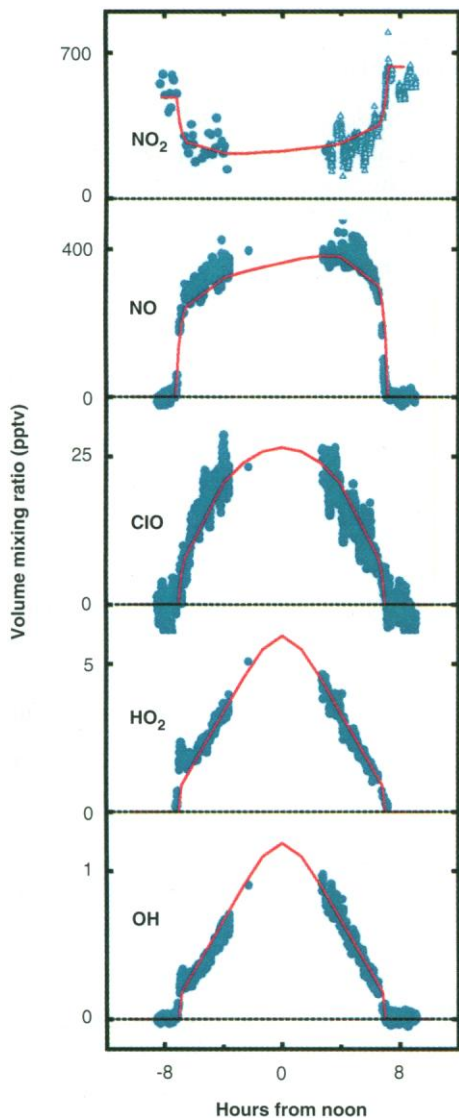


**Fig. 2.** Diurnal dependence of the concentrations of  $NO_2$ ,  $NO$ ,  $ClO$ ,  $HO_2$ , and  $OH$  all in pptv near 19 km. [ $NO_2$ ] measurements are shown from both the chemiluminescence instrument ( $\Delta$ ) and the laser-diode absorption instrument ( $\bullet$ ). The SPADE measurements were scheduled to coincide with the near null in stratospheric winds in order to sample essentially identical air masses on two subsequent days. In situ measurements of  $O_3$ ,  $CO_2$ ,  $H_2O$ , and  $N_2O$  confirm the dynamical and chemical similarity of the air sampled on 11 and 12 May 1993. Measurements made at other altitudes are removed by excluding data taken when the  $N_2O$  mixing ratio was greater than 260 or less than 220 ppbv. Lines are empirically derived functional forms of the diurnal dependence of the radical concentrations (see text for details).

from the JPL spectrometer are not available. Both instruments, however, recorded a consistently lower ratio of  $NO_2$  to  $NO$  than expected. The factor 0.7, an empirical correction based on analysis of the simultaneous measurements of  $NO$ ,  $NO_2$ ,  $ClO$ ,  $HO_2$ , and  $O_3$  concentrations, may result from errors in the calculated photolysis rate of  $NO_2$  or in the rate constant for the reaction of  $NO$  with  $O_3$  (17). As shown in Fig. 2, this model of the partitioning between  $NO_x$  and  $NO_3$  accurately describes the observed diurnal dependence of [ $NO$ ] and [ $NO_2$ ].

$ClO$  is produced primarily through the photolysis of chlorine nitrate,  $ClONO_2$ , at wavelengths both shorter and longer than the Huggins bands of  $O_3$  (320 nm). Photolysis over a broad spectral range gives rise to the more rounded shape for the diurnal variation of [ $ClO$ ], represented as the line in Fig. 2 by the empirical relation [ $ClO$ ]  $\propto$  [ $\cos(SZA)$ ] $^{1/2}$  for  $SZA < 90^\circ$ . Data taken near solar noon on other flights support this parameterization.

The time dependence of the odd-hydrogen radicals is driven primarily by the photolysis of  $HONO_2$  and  $O_3$  at wavelengths shorter than 310 nm (photolysis of  $O_3$  at these wavelengths produces  $O(^1D)$ , which subsequently reacts with  $H_2O$  or  $CH_4$  to produce  $OH$ ). The large optical depth of the atmosphere at these wavelengths (due to absorption by  $O_3$ ) gives rise to a stronger dependence on  $SZA$ , represented here by the empirical relation: [ $OH$ ] (or [ $HO_2$ ])  $\propto$  ( $100^\circ - SZA$ ) for  $SZA < 90^\circ$ . Data taken near solar noon on other flights support this parameterization (9).

Surprisingly, however, the  $OH$  concentration rose rapidly at sunrise despite the lack of appreciable radiation shortward of 310 nm. The sharp increase at sunrise is illustrated in Fig. 3 where  $OH$  and  $NO$  appear simultaneously at a  $SZA$  equal to  $90^\circ$ . Although most pronounced in the morning, this source of  $HO_x$  appears to occur throughout the day. Heterogeneous production of the readily photolyzed nitrous acid ( $HONO$ ) or similar species may be responsible (18). Photochemical models based on standard chemistry (19) fail to reproduce the  $OH$  concentration when the sun is near the horizon and thus underestimate the diurnally averaged concentration of  $OH$  and  $HO_2$  (16).

**Ozone photochemical removal and production rates.** Diurnally averaged removal rates for  $O_3$  were calculated using the  $SZA$ -dependent relations developed from the data taken on 11 and 12 May to infer the radical concentrations at all times of day. Removal rates for each catalytic cycle described below are equal to twice the net rate of the limiting reactions (reactions 4 through 9). The reaction rate constants for these processes were taken from the JPL evaluation (19). Removal and production rates of  $O_3$  calculated from the measured radical concentrations on 1 May 1993 are shown in Fig. 4.

Catalytic removal of  $O_3$  by the reactions:

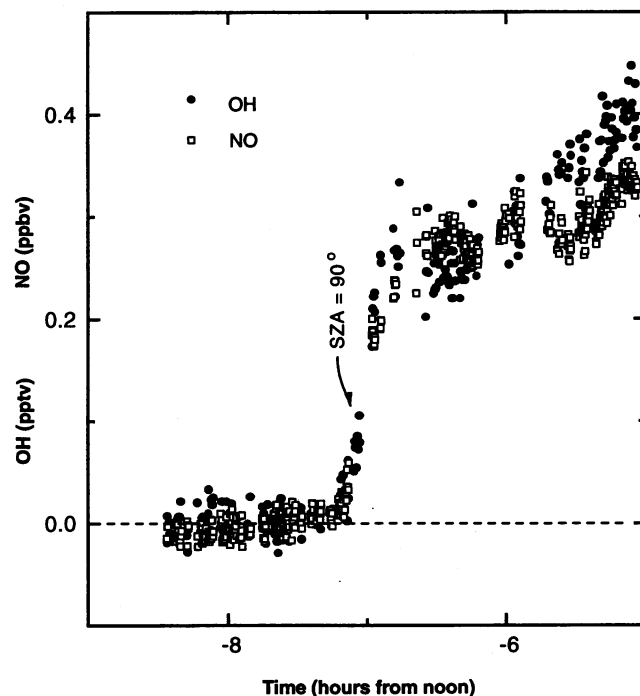
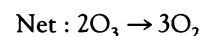
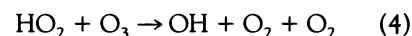
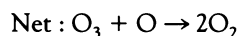
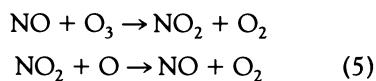


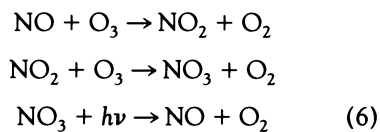
**Fig. 3.** [ $OH$ ] (pptv) and [ $NO$ ] (ppbv) measurements at sunrise on 11 May 1993.  $NO$ , produced by the photolysis of  $NO_2$  in the near UV, was expected to rise quickly at sunrise. The production of significant  $OH$  concentrations at this very high  $SZA$  was not expected. Photochemical models that use JPL (1992) chemistry (19) fail to reproduce this feature (16).

accounts for 30 to 50% of the total photochemical loss based on observed HO<sub>2</sub> concentrations. The reaction of OH + HO<sub>2</sub> → H<sub>2</sub>O + O<sub>2</sub> would then add an additional 5% to the loss ascribed to odd-hydrogen radical reactions.

In contrast to earlier models that predicted a much more important role for NO<sub>x</sub> catalysis, the cycles:



and

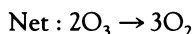
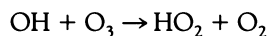
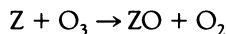
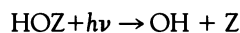


account for less than 20% of the total O<sub>3</sub> loss (*hν* represents a photon). Oxygen atom densities were calculated by assuming they are in photochemical steady state with:

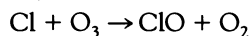
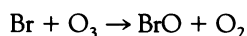
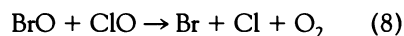
$$\text{O}_3 \cdot [\text{O}] = J_{\text{O}_3} [\text{O}_3] \div k_{\text{O} + \text{O}_2 \rightarrow \text{O}_3} [\text{O}_2]$$

Because [NO<sub>2</sub>] measurements were reported infrequently and for only some flights, we estimated its concentration from the measurements of [NO], [O<sub>3</sub>], [ClO], and [HO<sub>2</sub>] with the empirically modified photochemical steady-state expression (Eq. 2).

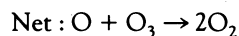
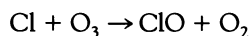
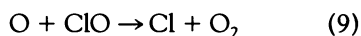
As a result of the rapid increase in the use of chlorofluorocarbons and halons during the last few decades, nearly one-third of the photochemical loss of O<sub>3</sub> is due to reactions involving ClO and BrO (20) radicals (based on observed concentrations of these radicals). The most important processes are:



where Z = Cl accounts for ~30% of the halogen-controlled loss and Z = Br accounts for between 20 and 30%. The reaction set



is responsible for 20 to 25% of the halogen-controlled loss. Finally,



accounts for 5% of O<sub>3</sub> loss by halogen chemistry at 15 km, increasing to 25% near 21 km. The formation of ClONO<sub>2</sub> and BrONO<sub>2</sub> leads to O<sub>3</sub> loss through photolysis to NO<sub>3</sub> followed by reaction 6 (21). These processes account for 10 to 15 percent of the halogen-controlled loss rates.

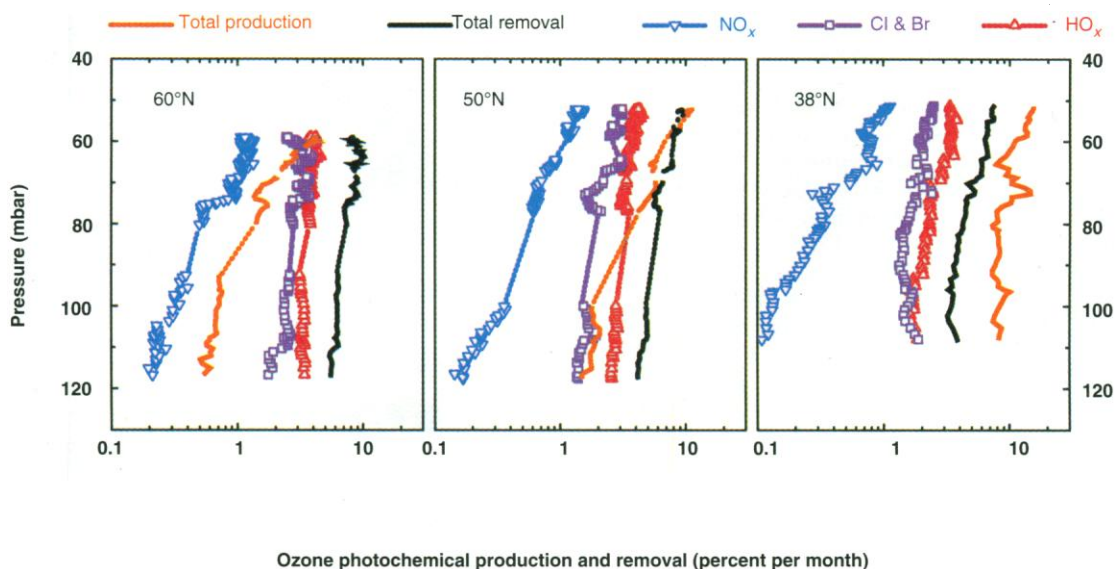
Production of O<sub>3</sub>, due primarily to the photolysis of oxygen at wavelengths <200 nm, exceeds photochemical loss at all latitudes less than 45°N during May (22). The latitudinal gradient in production is striking. Because of the large optical depths at these wavelengths, significant photolysis of oxygen does not occur until after the sun is ~45° above the horizon. As a result, pro-

duction of O<sub>3</sub> ceases in the northern latitudes (below 20 km) between the autumnal and vernal equinoxes. During the flight of 18 May 1993, 17 days after the flight represented in Fig. 4, production of O<sub>3</sub> at 60°N was greater than or equal to the loss at all altitudes between 15 and 21 km; the photolysis rate of oxygen had increased by nearly an order of magnitude at 60°N [see also Salawitch *et al.* (23)]. Removal rates, however, are much less sensitive to the minimum SZA; the total loss rates for O<sub>3</sub> shown in Fig. 4 are typical of the entire SPADE data set. Thus, net removal (loss – production) will be greatest in the spring and fall, when O<sub>3</sub> production is minimal and yet there remains sufficient sunlight to drive the radical chemistry. The measurements show that the time constant for photochemical removal of O<sub>3</sub> in the mid-latitude lower stratosphere during springtime can become short [net removal as fast as 8% removal per month (24)].

**Uncertainty in the O<sub>3</sub> removal rates.** Simultaneous measurements of the HO<sub>x</sub>, NO<sub>x</sub>, ClO, and BrO concentrations permit a relatively simple estimate of the accuracy of the calculated O<sub>3</sub> removal rates. Provided that reactions 4 through 9 account for all of the important loss processes, the uncertainty is a combination of the uncertainties in the free-radical measurements and the appropriate reaction rate constants determined in laboratory investigations. Such estimates are difficult to define in stratospheric models because of the nonlinear coupling between individual photochemical rates and the calculated radical concentrations.

We estimate that the uncertainty in the net rate of reaction 4, *k*<sub>4</sub>[HO<sub>2</sub>][O<sub>3</sub>], is less than a factor of 2. Although the HO<sub>2</sub> concentrations are accurate to ~25%, the JPL compendium suggests that uncertainty in the reaction rate constant for reaction 4, *k*<sub>4</sub>,

**Fig. 4.** Photochemical loss and production rates for O<sub>3</sub>. Measurements of the concentrations of OH, HO<sub>2</sub>, ClO, NO, and O<sub>3</sub> obtained during three altitude profiles on 1 May 1993 are used to infer the O<sub>3</sub> removal rates. The in situ measurements are scaled according to the observed diurnal profiles to obtain the integrated loss rates. The odd-hydrogen radicals were responsible for >40% of the photochemical loss in the lower stratosphere. The catalytic action of the halogen radicals accounted for nearly one-third of the total. Net removal of O<sub>3</sub> at the northernmost latitudes approached 10% per month.



is  $\times_{\pm 2.6}^{1.5}$  at the temperature of these measurements ( $\sim 210$  K) (19). Analysis of the measured ratio of OH to HO<sub>2</sub> by Cohen *et al.* suggests, however, that the rate of this reaction is within  $\times_{\pm 1.6}^{1.5}$  of the JPL recommended rate (25). Errors are likely to be systematic and therefore do not add in quadrature.

The calculated loss rates attributed to the halogens could be in error by as much as a factor of 2 to 3. Although the measured ClO concentrations are accurate to about 15 to 20% (26), the parameterization of the BrO concentration used in these calculations is uncertain ( $\pm 50\%$ ) (20). Furthermore, large uncertainties exist in the kinetics of the halogen and mixed halogen-odd hydrogen reactions. The JPL compendium suggests that the uncertainty in the reaction rate constant for reactions 7 (which account for one-half of the O<sub>3</sub> loss attributed to the halogens) is  $\times_{\pm 4.0}^{2.0}$  for chlorine and  $\times_{\pm 6.0}$  for bromine. The large uncertainty assigned to the BrO + HO<sub>2</sub> reaction results from the lack of experimental determination of the temperature dependence of the reaction rate. It seems very unlikely, however, that this reaction can proceed much faster than the nearly collision-rate limited reaction probability suggested by the JPL compendium (19). Additionally, analysis based on the measured HO<sub>2</sub> to OH ratio suggests that this reaction can proceed at a net rate ( $k_{\text{BrO}+\text{HO}_2}[\text{BrO}][\text{HO}_2]$ ) no faster than twice the rate used here. The BrO + ClO reaction (reaction 8) has  $\times_{\pm 1.65}$  uncertainty assigned to it. Finally, the kinetics of the O + ClO reaction are known to within  $\times_{\pm 1.3}$ . The predominant source of uncertainty is thus attributable to the lack of kinetic data at temperatures characteristic of the lower stratosphere (190 to 220 K).

We estimate that the calculation of the removal of O<sub>3</sub> due to NO<sub>x</sub> is accurate to within a factor of 1.8. The uncertainty in the rate of the reaction of O + NO<sub>2</sub> is driven largely by uncertainty in the concentration of O and NO<sub>2</sub>, because the reaction rate is known to within a factor of 1.25. The concentration of atomic oxygen is determined entirely by the O<sub>3</sub> photolysis and recombination rates. The formation rate (O + O<sub>2</sub> → O<sub>3</sub>) is known to within a factor of 1.25. The photolysis of O<sub>3</sub> at these altitudes is dominated by absorption in the Chappuis bands (450 to 800 nm), and the O<sub>3</sub> dissociation frequency will be sensitive to scattering, in particular albedo effects. The use of the TOMS reflectivity in the photolysis code to define the planetary albedo is thus very important in constraining the atomic oxygen densities to within a factor of 1.4. The NO<sub>2</sub> concentrations were determined by assuming photochemical steady state (Eq. 2) with the measured concentrations of NO, O<sub>3</sub>, ClO, and HO<sub>2</sub>. This relation has been shown to be accurate to within 30%

by direct measurements of [NO<sub>2</sub>].

The uncertainties in the O<sub>3</sub> removal rates at these altitudes are dominated by uncertainty in the laboratory-measured rate constants for reactions 4 through 9 at low temperature. The importance of establishing more firmly the ordering of the catalytic cycles underscores the need for further kinetic studies of these key reactions. Although we cannot conclusively demonstrate that the removal of O<sub>3</sub> by HO<sub>x</sub> is greater than that by ClO<sub>x</sub>, we do show that the sum of the rates of the odd hydrogen and halogen catalytic cycles is greater than the processes involving the nitrogen oxides. As discussed below, this ordering, in combination with the coupling of the radical families, determines the response of the O<sub>3</sub> removal rate to variations in the concentration of NO<sub>x</sub>.

**The role of NO<sub>x</sub>.** The SPADE measurements show the relatively minor role that NO<sub>x</sub> played in the direct removal of O<sub>3</sub> in April and May 1993. Because of the coupling that exists between [NO<sub>x</sub>] and the concentrations of the odd-hydrogen and halogen radicals, however, the rate of O<sub>3</sub> destruction in the lower stratosphere is still very sensitive to the concentrations of NO and NO<sub>2</sub>.

NO directly establishes the partitioning between OH and HO<sub>2</sub> through the reaction:



This process short-circuits the odd-hydrogen catalytic cycle (reactions 3 and 4) by reducing the concentration of HO<sub>2</sub>. The measured concentration of OH normalized to 30° SZA and the ratio of [HO<sub>2</sub>] to [OH] as a function of the NO mixing ratio is

shown in Fig. 5. Also shown is a model that describes the expected steady-state ratio (25):

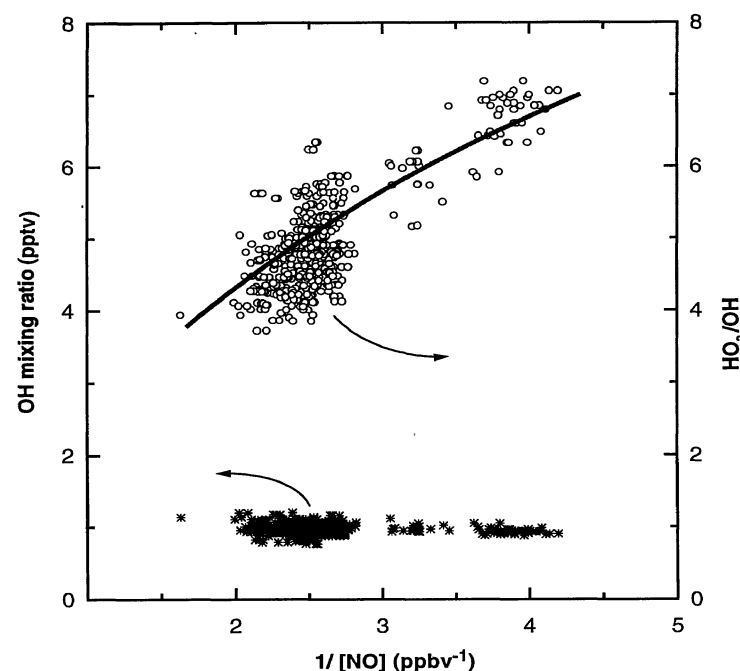
$$\frac{[\text{HO}_2]}{[\text{OH}]} \approx \frac{k_3[\text{O}_3]}{k_{10}[\text{NO}] + k_4[\text{O}_3]} \quad (11)$$

Figure 5 indicates that our understanding of the interaction of NO with HO<sub>x</sub> is qualitatively and quantitatively correct. Because the concentration of OH is largely independent of the concentration of NO, Eq. 11 describes the coupling of [HO<sub>2</sub>] and [NO<sub>x</sub>]. At constant [O<sub>3</sub>], the concentration of HO<sub>2</sub> will decrease with increasing [NO<sub>x</sub>], and thus the rates of reactions 4 and 7 will fall.

[NO<sub>x</sub>] and [ClO] are also strongly coupled through ClONO<sub>2</sub>. In steady state:

$$[\text{ClO}] = \frac{J_{\text{ClONO}_2}[\text{ClONO}_2]}{k_{\text{ClO}+\text{NO}_2}[\text{NO}_2]} \quad (12)$$

The rate of production of ClONO<sub>2</sub>,  $k_{\text{ClO}+\text{NO}_2}[\text{NO}_2][\text{ClO}]$ , is balanced by its photolytic destruction rate,  $J_{\text{ClONO}_2}$ . Decreases in the concentration of NO<sub>2</sub> lead directly to an increase in [ClO]. The observed concentration of ClO plotted versus  $J_{\text{ClONO}_2}[\text{Cl}_y] \div k_{\text{ClO}+\text{NO}_2}[\text{NO}_2]$  is shown in Fig. 6. Cl<sub>y</sub>, the total available inorganic chlorine ( $\sim \text{HCl} + \text{ClONO}_2$ ), has been determined from the measurements of the organic chlorine source gases as described by Woodbridge *et al.* (27). The line drawn through the data has a slope of 0.15, suggesting that in these air masses ClONO<sub>2</sub> is  $\sim 15\%$  of [Cl<sub>y</sub>] (28). To help ensure the similarity of the air masses, the data shown have been selected based on similar values of [N<sub>2</sub>O]. Additionally, to ensure that ClONO<sub>2</sub> and ClO are in steady state, only



**Fig. 5.** The measured OH concentration, normalized to 30° SZA, and the ratio of [HO<sub>2</sub>] to [OH] is plotted as a function of [NO] for O<sub>3</sub> mixing ratio of  $1.9 \pm 0.1$  ppmv. Included are all measurements when the pressure was  $65 \pm 2$  mbar, the temperature was within 3° of 212 K, and the SZA was  $< 80^\circ$ . The line is a model of the expected ratio as calculated from the in situ measurements (25). This ratio is set largely by the process that removes O<sub>3</sub> (reactions 3 and 4), and by the coupling of the odd-hydrogen and odd-nitrogen radicals (reaction 10).

data for which the SZA is  $<70^\circ$  are shown. The ClO concentrations respond to  $[\text{NO}_x]$  as predicted by Eq. 12. Stimpfle *et al.* show that these data are in consonance with earlier measurements made during the AASE II (September 1991 to March 1992) and SPADE test flight series (October and November 1992) (26).

The change in  $\text{O}_3$  loss rates in response to variations in  $[\text{NO}_x]$  for the mid-latitude lower stratosphere is shown schematically in Fig. 7. At  $[\text{NO}_x]$  values below some critical value (where  $\text{O}_3$  removal through the reaction of O with  $\text{NO}_2$  is equal to the sum of the loss processes due to the odd-hydrogen and halogen radicals), the loss rate of  $\text{O}_3$  increases with decreasing  $[\text{NO}_x]$ . Near this value, the rate of  $\text{O}_3$  loss is independent of the  $\text{NO}_x$  concentration because increases (or decreases) in  $[\text{NO}_x]$  result in comparable reductions (or enhancements) in the concentrations of  $\text{HO}_2$  and ClO. The addition of halogens to the stratosphere has shifted this buffered region to higher  $\text{NO}_x$  concentrations. At high  $[\text{NO}_x]$ , because of the predominance of nitrogen-radical catalysis, loss rates increase linearly with  $[\text{NO}_x]$ .

The nonlinear response of total  $\text{O}_3$  removal rates to changes in  $[\text{NO}_x]$  is reflected in the difficulty that assessment models have had in predicting the change in stratospheric  $[\text{O}_3]$  due to additions of halogens and reactive nitrogen species. For example, predictions for the change in  $[\text{O}_3]$  due to  $\text{NO}_x$  effluent from a hypothetical fleet of supersonic aircraft have oscillated wildly over the last 20 years—including changes in sign (29). The variability was driven largely by changes in the models' description of the relative importance of the reaction of atomic oxygen with  $\text{NO}_2$  compared with the reaction of  $\text{HO}_2$  with  $\text{O}_3$  and in the description of the coupling of the halogens and odd-hydrogen radicals to  $\text{NO}_x$ . The predicted ratio of  $[\text{HO}_2]$  to  $[\text{NO}_2]$  in the lower stratosphere, for example, has varied by an order of magnitude.

The SPADE measurements provide the first quantitative analysis of the radical-catalyzed removal of lower stratospheric  $\text{O}_3$  constrained by measurements of free-radical concentrations from each of the important chemical families:  $\text{HO}_x$ ,  $\text{ClO}_x$ ,  $\text{BrO}_x$ , and  $\text{NO}_x$ . This analysis shows the hierarchy of

the catalytic cycles and the dependence of  $\text{O}_3$  removal rates on the concentration of odd-nitrogen radicals in the lower mid-latitude stratosphere during May 1993. In all regions sampled,  $\text{NO}_x$  concentrations were sufficiently low that the total  $\text{O}_3$  loss rates were inversely correlated with  $[\text{NO}_x]$ .

Because the lifetime of  $\text{O}_3$  in the lower mid-latitude stratosphere is long compared with the rate of transport, however, the mixing ratio of  $\text{O}_3$  will reflect the photochemical history of the air mass.  $[\text{NO}_x]$  in the air mass will have varied considerably in response to numerous factors. In general,  $[\text{NO}_x]$  will be linearly proportional to the concentration of  $\text{NO}_y$ , which in turn is determined by the photochemical age of the air. (In the absence of aircraft effluent,  $\text{NO}_y$  is generated slowly in the stratosphere through the reaction of  $\text{O}^1\text{D}$  with  $\text{N}_2\text{O}$ .) In the lower stratosphere, the fraction of  $\text{NO}_y$  that exists in radical form ( $\text{NO}_x$ ) is governed primarily by the rate of  $\text{HONO}_2$  photolysis, processes involving OH, and the competition between the photolysis and aerosol-catalyzed hydrolysis of  $\text{N}_2\text{O}_5$ . In the absence of the Mt. Pinatubo aerosols (2 years earlier, for instance),  $\text{NO}_x$  concentrations would have been higher (likely by as much as 20 to 50%) and  $\text{O}_3$  removal rates would have been slower. Changes in  $[\text{NO}_x]$  of similar magnitude are predicted for variations in solar illumination for different latitudes, altitudes, or seasons.

In other regions of the stratosphere, we expect that the dependence of the  $\text{O}_3$  loss rates on  $[\text{NO}_x]$  will be qualitatively different from that represented in Fig. 7. At higher altitudes, partitioning within the odd-oxygen (O and  $\text{O}_3$ ) and odd-nitrogen families toward O and  $\text{NO}_x$  will result in substantially higher loss rates involving catalytic cycles in addition to reactions 4 through 9. During polar winter, the heterogenous conversion of the chlorine reservoir species HCl and  $\text{ClONO}_2$  into ClO can result in the complete removal of  $\text{NO}_x$  and rapid  $\text{O}_3$  loss through the self-reaction of ClO and reaction 8.

Further reductions in the uncertainty of assessments of the effects of perturbations in the concentrations of  $\text{NO}_x$ ,  $\text{NO}_y$ , or halogens will thus require: (i) simultaneous measurements of tracers, source gases, and free radicals—at higher altitudes, during different seasons, and under varying aerosol loading conditions; (ii) further laboratory investigation of the kinetics of the relevant photochemical reactions at low temperatures; and (iii) realistic parameterization of transport in the stratosphere (30).

## REFERENCES AND NOTES

1. Previous [NO] and [ClO] measurements made from the ER-2 [see, for example, J. C. King *et al.*, *Geophys. Res. Lett.* **18**, 2273 (1991); D. W. Fahey *et al.*,

**Fig. 6.**  $[\text{NO}_2]$  and [ClO] are coupled through chlorine nitrate,  $\text{ClONO}_2$ . The observed ClO concentration is plotted versus  $\beta/[\text{NO}_2]$ , where  $\beta = J_{\text{ClONO}_2}[\text{Cl}_y] / (k_{\text{ClO}+\text{NO}_2}[\text{Cl}_y] + k_{\text{ClO}+\text{NO}_2})$ .  $\text{Cl}_y$  is the total available inorganic chlorine (27). Data are shown where the SZA was  $<70^\circ$  and  $\text{N}_2\text{O}$  mixing ratios were  $230 \pm 20$  ppbv, for both the November SPADE test flights ( $\Delta$ ) and May ( $\bullet$ ) measurements. The slope of the line suggests that  $\text{ClONO}_2$  is  $\sim 15\%$  of  $\text{Cl}_y$  in these air masses.

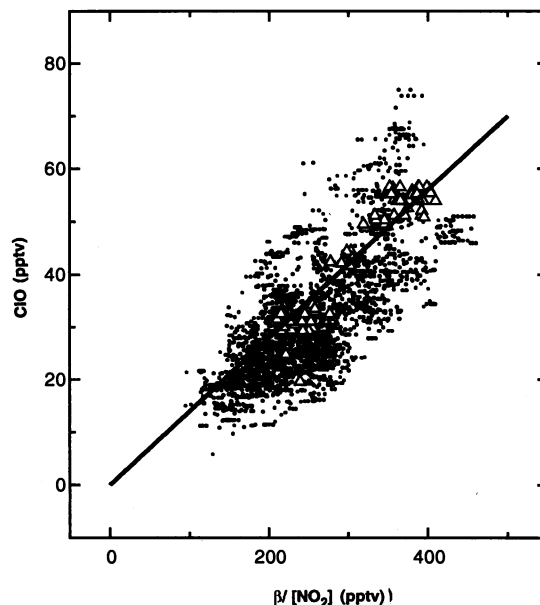
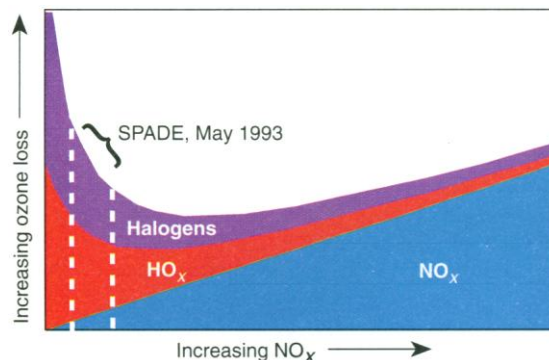


**Fig. 7.** The  $\text{O}_3$  removal rate is shown versus  $[\text{NO}_x]$ . Because of the coupling that exists between the radical families, the response of the total  $\text{O}_3$  removal rate to changes in  $[\text{NO}_x]$  is highly nonlinear. At sufficiently low  $[\text{NO}_x]$ , such as observed during the SPADE campaign, the removal rates are inversely correlated with  $[\text{NO}_x]$ .



- Nature* **363**, 509 (1993)] have shown significantly lower NO and higher ClO concentrations than had been predicted by models that did not include heterogeneous processes.
- The addition of a single reaction, the heterogeneous hydrolysis of N<sub>2</sub>O<sub>5</sub> (reaction 1), to the photochemical data set used in stratospheric models results in a shift away from an NO<sub>x</sub>-dominated lower stratosphere. In these models, NO<sub>x</sub> catalysis still dominates O<sub>3</sub> loss above 24 km. [See, for example, M. B. McElroy, R. J. Salawitch, K. Minschwaner, *Planet. Space Sci.* **40**, 373 (1992); J. M. Rodriguez *et al.*, *Geophys. Res. Lett.* **21**, 209 (1994), and references therein].
  - J. G. Anderson and O. B. Toon, *Geophys. Res. Lett.* **20**, 2499 (1993).
  - J. F. Gleason *et al.*, *Science* **260**, 523 (1993).
  - R. S. Stolarski and H. L. Wesoky, Eds., *NASA Ref. Publ. No. 1313* (1993).
  - D. R. Bates and M. Nicolet, *J. Geophys. Res.* **55**, 301 (1950).
  - The mixing ratio is the fraction of total molecules in a given volume. At the pressure and temperature typical of the ER-2 cruise altitude, there are approximately  $2 \times 10^{18}$  molecules cm<sup>-3</sup>. Thus, 1 pptv is equivalent to a concentration of  $2 \times 10^6$  molecules cm<sup>-3</sup>.
  - R. M. Stimpfle *et al.*, *Geophys. Res. Lett.* **17**, 1905 (1990).
  - P. O. Wennberg *et al.*, *Rev. Sci. Instrum.* **65**, 1858 (1994).
  - P. O. Wennberg *et al.*, unpublished results.
  - C. R. Webster, R. D. May, C. A. Trimble, R. G. Chave, J. Kendall, *Appl. Opt.* **33**, 454 (1994).
  - D. W. Fahey *et al.*, *J. Geophys. Res.* **94**, 11299 (1989); R. Gao *et al.*, *ibid.*, in press.
  - C. R. Webster *et al.*, *ibid.* **95**, 13851 (1990).
  - R. C. Cohen *et al.*, in preparation. The concentration of HONO<sub>2</sub>, which is required in this model, is inferred from the measurements of reactive nitrogen, NO<sub>y</sub>, by assuming:
 
$$[\text{HONO}_2] \approx [\text{NO}_y] - [\text{NO}] - [\text{NO}_2] - [\text{ClONO}_2]$$
 [ClONO<sub>2</sub>] is calculated by assuming photochemical steady state (Eq. 12). N<sub>2</sub>O<sub>5</sub> is neglected because of its small mixing ratio.
  - A photochemical steady state exists when the lifetime [concentration ÷ production (or loss) rate], is short; production is balanced by removal on short time scales. The radical species have short lifetimes, typically less than 1 hour, whereas some molecular species, such as HONO<sub>2</sub> or O<sub>3</sub> have lifetimes of months to years in the lower stratosphere.
  - R. J. Salawitch *et al.*, *Geophys. Res. Lett.*, in press.
  - L. Jaeglé *et al.*, *ibid.*, in press.
  - We speculate that an acid-catalyzed aerosol reaction of pernitric acid (PNA, HOONO<sub>2</sub>) could be a source of HONO. Although reactions of PNA on sulfuric acid aerosols have never been studied, Z. Li, R. R. Friedl, and S. P. Sander [in preparation] have shown that PNA is adsorbed on ice with high efficiency ( $\gamma = 0.15 \pm 0.10$  at 190 K). Salawitch *et al.*, show that an assumed  $\gamma$  of  $0.2 \pm 0.1$  results in an excellent match to the high zenith angle OH observations (16). This process increases the diurnally averaged HO<sub>x</sub> concentration in two ways: (i) it reduces an important sink (OH reacts quickly with PNA); and (ii) it redistributes HO<sub>x</sub> to high zenith angles, where its lifetime is longer. Additionally, this process would be a nonnegligible sink for O<sub>3</sub> in the lower stratosphere.
  - W. B. DeMore *et al.*, *Jet Propul. Lab. Publ. 92-20* (1992).
  - BrO is measured by the Harvard resonance fluorescence experiment [W. H. Brune, J. G. Anderson, K. R. Chan, *J. Geophys. Res.* **94**, 16639 (1989).] Because of the small BrO concentrations, long integration periods (typically 20 min or more) are required to achieve signal-to-noise ratios of greater than 2. We have used the [BrO] measurements from SPADE and the earlier AASE II campaign to develop a climatology. Measured BrO concentrations for all sunlit flights are consistent with the relation: [BrO] =  $0.45 (\pm 0.1) \times [\text{Br}_t]$ . Br<sub>t</sub> is the total available inorganic bromine (BrO + HOBr + BrONO<sub>2</sub> + HBr + Br) and is inferred from the measured [N<sub>2</sub>O] with the method

described by E. L. Woodbridge *et al.* for inorganic chlorine (27).

- R. Toumi, R. L. Jones, J. A. Pyle, *Nature* **365**, 37 (1993). For these calculations, we have used a quantum yield for NO<sub>3</sub> formation of 0.5, in line with the most recent laboratory work [see, for example, T. K. Minton, C. M. Nelson, T. A. Moore, M. Okumura, *Science* **258**, 1342 (1992)].
- Additional O<sub>3</sub> loss occurs through the reaction of O with O<sub>3</sub>. In addition to O<sub>2</sub> photolysis, production of O<sub>3</sub> occurs through the oxidation of CH<sub>4</sub> (and other hydrocarbons) in the presence of NO. These processes, although largely negligible, are included in the production and removal rates shown in Fig. 4.
- R. J. Salawitch *et al.*, *Geophys. Res. Lett.*, in press.
- This net removal rate can be compared with that inferred from Microwave Limb Sounder (MLS) ozone measurements. Under conditions of extreme chlorine activation, net removal rates in the arctic polar vortex during February 1993 (2 months before the measurements reported here) were estimated to be 20% per month [G. L. Manney *et al.*, *Nature* **370**, 429 (1994)].
- R. C. Cohen *et al.*, *Geophys. Res. Lett.*, in press.
- R. M. Stimpfle *et al.*, *ibid.*, in press.
- E. L. Woodbridge *et al.*, *J. Geophys. Res.*, in press. Correlations between the long-lived tracer N<sub>2</sub>O and organic chlorine compounds measured by gas chromatography (GC) are used to estimate the total organic chlorine and, by inference, the available inorganic chlorine. The GC measurements were made aboard the ER-2 during the SPADE and AASE II deployments by J. W. Elkins of the NOAA aeronomy laboratory. Additionally, whole air samples taken by S. M. Schauffler and L. E. Heidt of NCAR during AASE II included measurements of organic bromine compounds.
- This inference of the ClONO<sub>2</sub> concentration leads to difficulties in balancing the inorganic chlorine budget. In particular, measured HCl concentrations are usu-

ally lower than predicted by this estimate of the ClONO<sub>2</sub> concentration [see C. R. Webster *et al.*, *Science* **261**, 1130 (1993)].

- A. R. Douglass *et al.*, *NASA Ref. Publ. No. 1251* (1991).
- In situ measurements of the distribution of long-lived tracers such as those made during SPADE can be used to place constraints on dynamical transport rates, a key issue in determining the distribution and lifetime of O<sub>3</sub> [K. A. Boering *et al.*, *Geophys. Res. Lett.*, in press; S. C. Wofsy *et al.*, *ibid.*, in press; E. Hintsas *et al.*, *ibid.*, in press].
- We thank the pilots (W. Collette, J. Barrilleaux, D. Krumrey, J. Nystrum, and R. Williams) and the ground crews of the ER-2, without whom this work would not have been possible. ER-2 flight planning by P. A. Newman and co-workers from NASA-Goddard was instrumental to the success of SPADE. The TOMS UV reflectivity is produced by R. D. McPeters and co-workers of the NASA-Goddard ozone processing team; L. Pfister at NASA-Ames was responsible for interpolating this data onto the ER-2 flight track. New instrumentation for OH and HO<sub>2</sub> was developed in part by N. L. Hazen, L. B. Lapson, N. T. Allen, J. F. Oliver, N. W. Lanham, J. N. Demusz, E. E. Thompson, T. L. Martin, E. M. Weinstock, and A. E. Dessler at Harvard University. Interface with the ER-2 was supported by H. Kent, G. Prince, and R. York, at Lockheed; their efforts are gratefully acknowledged. Program support at NASA-Ames by J. C. Arveson, J. L. Barrilleaux, E. Condon, S. Wegner, and S. Hipskind is acknowledged. Finally, this work was supported by the NASA High Speed Research Program, under the direction of H. L. Wesoky, R. S. Stolarski, and M. J. Prather. Additional support for the HO<sub>x</sub> instrument development came from the NASA Upper Atmosphere Research Program, under the direction of M. J. Kurylo.

6 June 1994; accepted 1 September 1994

# TLC1: Template RNA Component of *Saccharomyces cerevisiae* Telomerase

Miriam S. Singer and Daniel E. Gottschling

Telomeres, the natural ends of linear eukaryotic chromosomes, are essential for chromosome stability. Because of the nature of DNA replication, telomeres require a specialized mechanism to ensure their complete duplication. Telomeres are also capable of silencing the transcription of genes that are located near them. In order to identify genes in the budding yeast *Saccharomyces cerevisiae* that are important for telomere function, a screen was conducted for genes that, when expressed in high amounts, would suppress telomeric silencing. This screen led to the identification of the gene *TLC1* (telomerase component 1). *TLC1* encodes the template RNA of telomerase, a ribonucleoprotein required for telomere replication in a variety of organisms. The discovery of *TLC1* confirms the existence of telomerase in *S. cerevisiae* and may facilitate both the analysis of this enzyme and an understanding of telomere structure and function.

Telomeres are specialized nucleoprotein complexes that constitute the ends of eukaryotic chromosomes and protect chromosomes from degradation and end-to-end fusion (1, 2). When telomeres are absent, the instability of nontelomeric chromosomal

ends leads to chromosome loss (3). In addition, telomeres are required for the complete replication of chromosomes (1, 2, 4).

DNA polymerases synthesize DNA in a 5' to 3' direction and require a primer to initiate synthesis. These restrictions pose a problem for the complete replication of linear chromosomes (5). In the absence of a specialized mechanism to maintain termi-

The authors are in the Department of Molecular Genetics and Cell Biology, The University of Chicago, Chicago, IL 60637, USA.